

Title Page

Pharmacokinetic-Pharmacodynamic Modeling of Brain Dopamine Levels based on
Dopamine Transporter Occupancy after Administration of Methylphenidate in Rats

Ryosuke Shimizu, Naotaka Horiguchi, Koji Yano, Masashi Sakuramoto, Naoki
Kanegawa, Shunji Shinohara, and Shuichi Ohnishi

Clinical Pharmacology and Pharmacokinetics (R.S.), Neuroscience Drug Discovery &
Disease Research Laboratory (N.H., K.Y), and Drug Metabolism & Pharmacokinetics
(M.S., N.K., S.O.), Shionogi & Co., Ltd., Osaka, Japan.

Technology for Animal Models (S.S.), Shionogi TechnoAdvanced Research Co., Ltd.,
Osaka, Japan.

Running Title Page

Running Title: Dopamine PK-PD Model of Methylphenidate

Corresponding author: Ryosuke Shimizu

Address: Umeda Office, Shionogi & Co., Ltd.

12F, Hankyu Terminal Bldg., 1-4 Shibata 1-chome, Kita-ku, Osaka 530-0012, Japan

Tel: +81-6-6485-5088, Fax: +81-6-6475-5780

E-mail: ryosuke.shimizu@shionogi.co.jp

The number of text pages: 52

The number of tables: 4

The number of figures: 8

The number of references: 32

The number of words in the Abstract: 246

The number of words in the Introduction: 745

The number of words in the Discussion: 1483

Abbreviations

ADHD, Attention Deficit Hyperactivity Disorder

AUC, area under the plasma concentration-time curve

CNS, central nervous system

CSF, cerebrospinal fluid

DAT, dopamine transporter

dAUE, the change of the area under the effect-time curve

ECF, extracellular fluid

FLIPR, fluorometric imaging plate reader

HPLC-MS/MS, high performance liquid chromatography–tandem mass spectrometry

k_{off} , dissociation rate constant for DAT

k_{on} , association rate constant for DAT

NAc, nucleus accumbens

NET, norepinephrine transporter

PK-PD, pharmacokinetic-pharmacodynamic

A recommended section assignment to guide the listing in the table of contents:

Neuropharmacology

Abstract

Dopamine exerts various effects including movement coordination and reward. It is useful to understand the quantitative relationship between drug pharmacokinetics and target engagement such as the change of occupancy and dopamine level in brain for the proper treatment of dopamine-related diseases. This study was aimed at developing a pharmacokinetic-pharmacodynamic (PK-PD) model based on dopamine transporter (DAT) occupancies that could describe changes in extracellular dopamine levels in brain after administration of methylphenidate (DAT inhibitor) to rats. First, uptake of fluorescent substrates was studied in DAT expressing human embryonic kidney 293 cells and concentration dependently inhibited by methylphenidate. By analyzing the uptake of fluorescent substrates in the presence or absence of methylphenidate, a mathematical model could estimate the association and dissociation rate constants of methylphenidate for DAT. Next, we measured the concentrations of methylphenidate in plasma and cerebrospinal fluid (CSF) and extracellular dopamine levels in the nucleus accumbens after a single intraperitoneal administration of methylphenidate. The concentrations of methylphenidate in plasma increased almost dose-proportionally and the CSF-to-plasma concentration ratio was similar among evaluated dose. The extracellular dopamine levels also increased with dose. These data were analyzed using

the mechanism-based PK-PD model which incorporates dopamine biosynthesis, release from a synapse, reuptake *via* DAT into a synapse, and elimination from a synapse. Methylphenidate concentrations in plasma and dopamine profiles predicted by the PK-PD model were close to in vivo observations. In conclusion, our mechanism-based PK-PD model can accurately describe dopamine levels in the brain after administration of methylphenidate to rats.

Introduction

Mechanism-based pharmacokinetic-pharmacodynamic (PK-PD) modeling has provided useful information to understand the quantitative relationship between drug concentrations and target engagements or pharmacological effects (Visser et al., 2017). For the central nervous system (CNS) acting drugs, biomarker responses and target receptor occupancy are used as indexes of target engagements for the therapeutic effect. In general, a mechanism-based PK-PD model has been developed based on data from animal experiments and in vitro assay because the availability of human biomarker responses in target tissue is limited. Yassen et al. (2006) described a different efficacy profile of buprenorphine and fentanyl using the PK-PD model based on the association and dissociation rate constants (k_{on} and k_{off}) for opioid mu receptor because it is well established that buprenorphine displays slow receptor association/dissociation kinetics in vitro as well as in vivo, causing a slow onset and a long duration of the effect. Zuideveld et al. (2007) and Johnson et al. (2016) have also reported the prediction of human 5-HT_{1A} receptor mediated responses and dopamine D₂ receptor occupancy from preclinical PK-PD models. Establishing mechanism-based PK-PD modeling using preclinical information of biomarker responses and target receptor occupancy could offer a mechanistic basis of the drugs acting into CNS, and eventually enable to

consider proof of concept and optimal dosage design.

Dopamine plays an important role as a neurotransmitter in pathophysiological processes. Meiser et al. (2013) summarized the dopamine biosynthesis and metabolism processes. Briefly, (i) dopamine is synthesized by the combined action of tyrosine hydroxylase and aromatic amino acid decarboxylase in the neurites of dopaminergic neurons and imported into synaptic vesicles, (ii) on neuronal excitation, dopamine is released into the synaptic cleft for signal transduction, (iii) dopamine is taken into dopaminergic neurons *via* the dopamine transporter (DAT), and (iv) dopamine is metabolized to norepinephrine by dopamine β -hydroxylase or degraded by monoamine oxidase and catechol-*O*-methyltransferase in dopaminergic neurons. There are five different dopamine receptors, and dopamine exerts various effects including movement coordination, reward, cognition and emotion by stimulating these receptors (Moraga-Amaro et al., 2016). Dopamine-related diseases such as Attention Deficit Hyperactivity Disorder (ADHD), Parkinson disease, and dementia with Lewy bodies respectively show various physical and mental symptoms mainly due to dopamine dysfunction (Mereu et al., 2017), progressive loss of dopaminergic neurons (Ammal et al., 2018) and accumulation of Lewy bodies (Colom-Cadena et al., 2017). Drugs that regulate the dopamine level or its function in the brain have been used to treat these

diseases. However, an imbalance in dopamine also causes many side effects, and therefore, quantitatively understanding its relationship between drug pharmacokinetics and target engagements gives useful information to consider the therapeutic outcome.

ADHD is one of the most common neurobehavioral disorders in childhood (Briars et al., 2016). Amphetamine and methylphenidate are widely used as stimulant drugs for ADHD treatment. Methylphenidate inhibits both DAT and norepinephrine transporter (NET) (Briars et al., 2016) and increases dopamine in the striatum and nucleus accumbens (NAc). According to Bymaster et al. (2002), atomoxetine, which is a NET inhibitor, did not increase dopamine in the striatum and NAc, suggesting that methylphenidate predominantly increases dopamine in the striatum and NAc through DAT inhibition. In contrast, the pharmacological action of amphetamine is mediated by a complex mechanism including promotion of dopamine release from the dopaminergic synapse in addition to DAT inhibition (Briars et al., 2016). As the pharmacological mechanism of methylphenidate has been well profiled compared to amphetamine, methylphenidate was chosen as a reference drug to establish a mechanism-based PK-PD model to accurately understand the correlation between dopamine behavior and DAT inhibition. Aoyama et al. (1997) has reported on PK-PD analysis to obtain a dopamine profile after administration of methylphenidate to rat. They analyzed the dopamine

profile assuming competitive inhibition of DAT by extracellular methylphenidate concentration in the brain. However, this model did not consider the k_{on} and k_{off} of methylphenidate to DAT, and therefore is not applicable to the efficacy profile characterized by slow binding kinetics, such as buprenorphine. In the present study, we focused on the dopamine profile, k_{on} and k_{off} of methylphenidate to DAT were calculated using a mathematical model based on the mechanism of in vitro fluorescence-based uptake study for DAT, and these values were incorporated into the PK-PD model to simulate the dopamine profile after administration of methylphenidate. Our objective was to investigate the mechanism-based approach to develop a PK-PD model to describe the change of dopamine levels by DAT inhibition after administration of methylphenidate to rats using DAT occupancy derived from k_{on} and k_{off} values of methylphenidate.

Materials and Methods

Materials and Reagents.

Methylphenidate hydrochloride (racemic form) was purchased from Sigma-Aldrich Japan, Inc. (Tokyo, Japan). Cocaine was purchased from Takeda Pharmaceutical Company Limited (Osaka, Japan). Fluorescent-based Neurotransmitter Transporter Uptake Assay dye was obtained from Molecular Devices (Sunnyvale, CA). Saline was purchased from Otsuka Pharmaceuticals (Tokyo, Japan). All other reagents and solvents were commercial products of reagent grade.

Animals

Animal care and all experimental procedures were performed with the approval of the Institutional Animal Care and Use Committee of Shionogi in terms of the 3R (Replacement/Reduction/Refinement) principles. Male Crlj:WI rats were purchased at 5 weeks of age from Charles River Laboratories Japan, Inc. (Yokohama, Japan). After quarantine for a week, the rats were acclimated for several days in the animal compartment. The rats were used for the experiments at 6 weeks of age. During the acclimation and experimental periods, the rats were placed under the conditions of room temperature of 20-26°C, relative humidity of 30-70%, and lighting for 12 hr (light

[8:00-20:00]/dark [20:00-8:00]) and allowed free access to tap water and solid laboratory food (CE-2, CLEA Japan, Inc.).

Fluorescence-based uptake Study

Methylphenidate was dissolved in assay buffer (Hank's Balanced Salt solution containing 20 mM HEPES, 0.1% bovine serum albumin, pH 7.3) to prepare the methylphenidate solution at 0.0781-2.50 μ M. Neurotransmitter assay loading dye reagent (DAT substrate) was dissolved in Hank's Balanced Salt solution containing 20 mM HEPES to prepare the loading buffer. Human embryonic kidney 293 cells stably transfected with human recombinant DAT were seeded at a density of 1×10^5 cells/ml (50 μ L/well) in 384-well, clear-bottomed, black-walled plates (Greiner Bio-one[®], Cat. #781090, Frickenhausen, Germany) and allowed to proliferate overnight. On the day of the experiment, the culture medium was aspirated from the cell plate using a plate washer followed by addition of 20 μ L assay buffer. After the plate was placed in the fluorometric imaging plate reader (FLIPR), the cells were incubated at room temperature for 5 min to capture the fluorescence at baseline. Next, both 10 μ L of loading buffer and 10 μ L of methylphenidate solution were added the cells cultured on a 384-well plate, and the cells were incubated at room temperature for 90 minutes. During

the incubation, fluorescence was measured at every 3 seconds for the first 3 min and every 10 seconds for the residual 87 min (total points were 580 per concentration). To measure fluorescence, the dye was excited using light at a wavelength of 470-495 nm, and emission was collected at 515-575 nm. The same study was performed with cocaine (0.313 and 0.625 μ M), which has the potential of DAT inhibition (Gatley et al., 1996) to support the validity of our mathematical model. The fluorescence strengths were represented the mean of duplicated data.

Pharmacokinetic Study

Rats were anesthetized with isoflurane, and a cannula was inserted into the jugular vein 4 days before the pharmacokinetic study. Methylphenidate dissolved in saline was intraperitoneally administered to conscious rats ($n = 3-5/\text{dose}$) at dose of 1, 3, and 6 mg/2 mL/kg using a 1-mL syringe with a 25-gauge needle. Blood (approximately 0.2 mL) was collected from the inserted cannula using a 1-mL syringe with a 23-gauge needle containing heparin and EDTA-2K at 0.033, 0.083, 0.25, 0.5, 1, 2, and 4 hours after administration. To other rats, methylphenidate solution was intraperitoneally administered ($n = 3/\text{dose}$) at dose of 1, 3, and 6 mg/2 mL/kg to measure the brain and CSF concentration of methylphenidate. The concentrations in brain were evaluated for

brain penetration and the concentrations in CSF were evaluated for unbound concentration in brain. CSF was collected by inserting a 23-gauge needle connected to a syringe through a polyethylene tube into the cisterna magna at 30 min after collection of whole blood *via* the inferior vena cava. The brain was also collected from the same rats. The collected whole blood was centrifuged at 1600 g for 10 min at 4°C to obtain plasma. The polyethylene tube for CSF sampling was washed with an equal amount of acetonitrile to prevent adsorption of the compound to the tube. Water was added to the brain samples at a ratio of brain/water = 1/3 (v/v), and the samples were homogenized. The obtained plasma, CSF and brain samples were frozen and stored at -30°C until analysis. Methylphenidate in plasma and brain samples was extracted with acetonitrile and centrifugal separation (5000 rpm for 5 min at 8°C), and each supernatant was injected to high performance liquid chromatography/tandem mass spectrometry (HPLC-MS/MS) using API4000 (SCIEX, Foster City, CA, USA). The range of calibration standards was 0.5-5000 ng/mL for plasma and brain samples and 0.15-1500 ng/mL for CSF samples.

In vivo Microdialysis Study for Dopamine Release in Nucleus Accumbens

Rats were anesthetized with sodium pentobarbital (40 mg/kg, i.p.) and butorphanol

(5 mg/kg, s.c.), and a dialysis probe (EicomCorp., Kyoto, Japan) with a guide cannula was stereotaxically implanted at the NAc shell of each rat (A +1.8 mm, L +0.8 mm, V +6.2 mm, from the bregma and skull) (Paxinos and Watson, 1986). The cannula was cemented in place with dental acrylic, and the animal was kept warm and allowed to recover from anesthesia. Postoperative analgesia was performed by a single injection of buprenorphine (0.02 mg/kg, i.p.) (Ago et al., 2006; Sato et al., 2007). The active probe membranes were 2 mm long. Two or three days after surgery, the probe was perfused with Ringer's solution (147.2 mM NaCl, 4.0 mM KCl, and 2.2 mM CaCl₂; pH 6.0; Fuso Pharmaceutical Industries, Ltd., Osaka, Japan) at a constant flow rate of 2 μ L/min and stabilized for 5 hours. Next, after methylphenidate solution had been intraperitoneally administered to conscious rats (n = 4/dose) at dose of 1, 3, and 6 mg/2 mL/kg, microdialysis samples (12 μ L) were collected every 6 min over 240 min and immediately injected to HPLC analysis to determine the dopamine level, as previously reported (Ago et al., 2011; Koda et al., 2010). After the experiments, Evans Blue dye was microinjected through the cannula to histologically verify the position of the probe. Only data from animals with the correct probe placements were used for the analysis.

In vitro Mathematical Model

Figure 1 presents the scheme of the in vitro kinetic assay. The concentrations of fluorescent substrates (C_{sub}) and fluorescence strength (C_{flu}) profiles were described by the following equations (1) and (4):

$$dC_{sub}/dt = -k'_{on} \cdot C_{sub} \cdot DAT_{free} \quad (1)$$

$$dC_{flu}/dt = k'_{on} \cdot C_{sub} \cdot DAT_{free} \quad (2)$$

$$dDAT_{free}/dt = -k_{on} \cdot C_{inh} \cdot DAT_{free} + k_{off} \cdot DAT_{bound} \quad (3)$$

$$dDAT_{bound}/dt = k_{on} \cdot C_{inh} \cdot DAT_{free} - k_{off} \cdot DAT_{bound} \quad (4)$$

where, k'_{on} is the permeability rate constant of the fluorescent substrates; DAT_{free} is unbound fraction of DAT; DAT_{bound} is bound fraction of DAT by DAT inhibitor; k_{on} and k_{off} are the association and dissociation rate constants of DAT inhibitor; and C_{inh} is the concentration of DAT inhibitor (μM). The initial values of DAT_{free} and DAT_{bound} are 1 and 0, respectively.

This analysis is based on two hypotheses: (i) fluorescence strength is equal to the concentration of fluorescent substrates which penetrate through DAT and (ii) at steady state, all substrates are transported *via* DAT (C_{sub} at $t = 0$ is considered the maximum fluorescence strength).

In the absence of DAT inhibitor (Figure 1[a]), DAT_{free} was set as 1 constantly because there was no inhibitor for DAT, as fluorescent substrates mainly penetrate *via*

all DAT into the cells and produce fluorescence. Therefore, C_{sub} and C_{flu} profiles were described by the equations (1) and (2), and both C_{sub} and k'_{on} were estimated by a fitting approach based on the observed fluorescence strength profiles.

In the presence of DAT inhibitor (Figure 1[b]), fluorescent substrates penetrate *via* only the free DAT into the cells and produce fluorescence. Therefore, the changes of C_{sub} , C_{flu} , and DAT occupancy were described by the equations (1) to (4). The k_{on} and k_{off} of the DAT inhibitor were estimated by a fitting approach based on the observed fluorescence strength profiles.

Mechanism-based PK-PD Model

Figure 2 presents the structure of the mechanism-based PK-PD model for dopamine levels in rat brain after intraperitoneal administration of methylphenidate. Our PK-PD model was developed based on following four points: (i) 2-compartment model for plasma concentration of methylphenidate; (ii) a compartment for CSF concentration of methylphenidate attached to the plasma compartment; (iii) a component for DAT occupancy calculated with the concentration in CSF of methylphenidate, k_{on} , and k_{off} ; (iv) a model incorporating dopamine biosynthesis, release from a synapse, reuptake *via* free DAT into the synapse and elimination from the synapse. The concentrations of

methylphenidate in plasma and CSF were described by a linear two-compartment model as follows:

$$dA_{ip}/dt = -k_a \cdot A_{ip} \quad (5)$$

$$dA_{central}/dt = k_a \cdot A_{ip} - k_e \cdot A_{central} - k_{12} \cdot A_{central} + k_{21} \cdot A_{peri} \quad (6)$$

$$dA_{peri}/dt = k_{12} \cdot A_{central} - k_{21} \cdot A_{peri} \quad (7)$$

$$C_{plasma} = A_{central}/(V_d/F) / MW * 1000 \quad (8)$$

$$C_{CSF} = C_{plasma} \times Kp_CSF \quad (9)$$

where A_{ip} , $A_{central}$ and A_{peri} are the methylphenidate amount (mg/kg) in the abdominal cavity, central and peripheral compartment, respectively; F is bioavailability; V_d/F is the distribution volume corrected by F of methylphenidate in the central compartment (L/kg); k_a , k_{12} , k_{21} and k_e are the first-order rate constants of absorption from the injection site, distribution to a peripheral or the central compartment, and elimination from the central compartment (/min), respectively; MW is the molecular weight of methylphenidate (233 g/mol); C_{plasma} is the concentration of methylphenidate in plasma (μM). Kp_CSF is the CSF-to-plasma concentration ratio, and C_{CSF} is the concentration of methylphenidate in CSF.

To analyze the dopamine levels in the brain, DAT occupancy was described as equation (10) and dopamine levels in a synapse were described by equations (11) and

(12):

$$dDAT_{RO}/dt = k_{on} \times C_{CSF} \times (1 - DAT_{RO}) - k_{off} \times DAT_{RO} \quad (10)$$

$$dDA_{pre}/dt = k_{syn} - k_{release} \times DA_{pre} + k_{reuptake} \times DA_{post} \times (1 - DAT_{RO})^\gamma - k_{deg} \times DA_{pre} \quad (11)$$

$$dDA_{post}/dt = k_{release} \times DA_{pre} - k_{reuptake} \times DA_{post} \times (1 - DAT_{RO})^\gamma \quad (12)$$

where DAT_{RO} is the fraction of DAT occupied by methylphenidate in the brain; k_{on} and k_{off} are in vitro association and dissociation rate constants of methylphenidate for DAT, respectively; DA_{pre} and DA_{post} are dopamine levels in presynapse and extracellular space. DA_{pre_0} and DA_{post_0} , which are initial values of DA_{pre} and DA_{post} , are $DA_{post_0} \times k_{uptake}/k_{release}$ ($= k_{uptake}/k_{release}$) and 1 (100%), respectively; k_{syn} is the zero-order rate constant for dopamine biosynthesis and $k_{syn} = k_{deg} \times DA_{pre_0}$; $k_{release}$, k_{uptake} and k_{deg} are first-order rate constants for dopamine release from presynapse to extracellular space, dopamine reuptake from extracellular space to synapse and degradation from synapse, respectively; γ is hill coefficient.

Data Analysis

Pharmacokinetic analysis for the concentration of methylphenidate in plasma was performed based on a non-compartment model with uniform weighting. The area under

the plasma concentration–time curve from time zero to infinity (AUC_{inf}) was calculated by the trapezoidal rule. The other pharmacokinetic parameters were as follows: maximum plasma concentration (C_{max}), time to reach maximum plasma concentration (T_{max}). Pharmacodynamic analysis of dopamine level per time was also performed based on the non-compartment model with uniform weighting. The change of the area under the effect-time curve for dopamine level from time zero to the last time ($dAUE_{all}$) was calculated by the trapezoidal rule. Maximum dopamine level (L_{max_d}) and time to reach maximum dopamine level (T_{max_d}) were also calculated.

The k_{on} and k_{off} of DAT inhibitors were estimated based on the mean data of duplication. The model-dependent PK and PK-PD parameters were estimated by individual data for all doses to obtain the unique estimates for all parameters. To the process of PK-PD modeling, a sequential pharmacokinetic and pharmacodynamic modeling approach was applied, i.e., first the pharmacokinetic modeling was conducted, and then PK-PD modeling was performed using pharmacokinetic parameters estimated from the pharmacokinetic model to find the mean concentrations of methylphenidate in plasma.

Model-independent pharmacokinetic parameters and all model-dependent parameters were estimated using Phoenix WinNonlin (ver. 6.2.1, Pharsight Corp.).

Model-independent pharmacodynamic parameters were calculated using Microsoft Excel 2010. Dose-proportionalities were evaluated using SAS (ver. 9.2) and power model for ln-transformed C_{\max} and AUC_{inf} .

Results

Estimation of k_{on} and k_{off} by in vitro transport study of DAT substrates

The observed fluorescent strength profiles of DAT substrates in the absence or presence of methylphenidate (0.0781-2.50 μM) are represented in Figure 3. Fluorescent strengths of DAT substrates increased with the time and reduced by methylphenidate in a concentration dependent manner. These observed data showed good fit with the equations (1) to (4) and the fitting analysis resulted in the estimation of k'_{on} , C_{sub} , k_{on} and k_{off} with CV values of less than 5% (Table 1). The dissociation constant (K_d) of methylphenidate was also calculated by k_{off}/k_{on} and represented in Table 1. As k_{on} and k_{off} values were similar at all concentrations of methylphenidate, k_{on} (1.24 / $\mu\text{M}/\text{min}$) and k_{off} (0.129 /min) values at 0.313 μM were selected for PK-PD modeling. The K_d value (104 nM) of methylphenidate was comparable to reported values (K_i values of 84 ± 33 nM from Gatley et al., 1996 and 109 nM from Slusher et al., 1997). To confirm the validity of the model, k_{on} and k_{off} values of cocaine were also evaluated. The time-courses of observed fluorescent strength of DAT substrates in the absence or presence of cocaine (0.313 and 0.625 μM , respectively) are presented in Figure 4 and the estimated parameters of cocaine in Table 1. The model well described the change of fluorescent strength and provided k_{on} and k_{off} with CV values of less than 1.67%. The

calculated K_d values for cocaine at 0.313 and 0.625 μM were 250 and 261 nM, respectively, which were close to the reported values (K_i values of 120 nM from Gatley et al., 1996 and 210 nM from Slusher et al., 1997). These results indicated that k_{on} and k_{off} values of the DAT inhibitor could be estimated by the model which can describe the observed fluorescent strength of DAT substrates in the absence or presence of DAT inhibitor.

Pharmacokinetic and Pharmacodynamic Properties of Methylphenidate in Wistar Rats

The concentration profiles of methylphenidate in plasma after an intraperitoneal administration of methylphenidate at 1, 3, and 6 mg/kg are presented in Figure 5 and the calculated pharmacokinetic parameters of methylphenidate are listed in Table 2. Methylphenidate was rapidly absorbed and showed biphasic decline with time from plasma. From the results of evaluation of dose-proportionality, the slope of regression and 95% confidence intervals for C_{max} were 1.13 and 0.95-1.30 and those for AUC_{inf} were 1.25 and 1.15-1.36, therefore C_{max} increased almost in a dose-proportional manner but AUC_{inf} increased more than dose-proportionality. With intraperitoneal administration at 1, 3, and 6 mg/kg, the K_p_{brain} (brain-to-plasma ratio) and K_p_{CSF}

(CSF-to-plasma ratio) were 10.6-11.2 and 1.20-1.66, respectively, which are more than 1.0 and constant regardless of the dose. These results suggested that brain distribution of methylphenidate was high and within dose-linearity up to 6 mg/kg. The dopamine profiles in NAc after intraperitoneal administration of methylphenidate at 1, 3, and 6 mg/kg are presented in Figure 6 and each pharmacodynamic parameter is listed in Table 3. There were large inter-individual variations, especially at a low dose. T_{\max_d} values of dopamine (16.5-25.5 min) were delayed compared to those of methylphenidate concentrations in plasma (2.0 – 2.6 min). Furthermore, L_{\max_d} and $dAUE_{\text{all}}$ increased in a dose-dependent manner.

PK-PD Modeling for Dopamine Response

For pharmacokinetic profiles, a linear two-compartment model with first-order absorption was selected although AUC_{inf} increased more than dose-proportionality because the slope of regression was not so large, and the model well described the concentration of methylphenidate in plasma (Figure 5) with reasonable variability in the estimated parameters (CV: 7.34-38.5%, Table 4). The concentrations of methylphenidate in CSF were calculated with the concentration in plasma and K_p_{CSF} (equation (9)), which used the averaged value from 9 rats because there was little

variability among individuals and doses. The time-course of calculated DAT occupancies after intraperitoneal administration of methylphenidate at 1, 3, and 6 mg/kg are presented in Figure 7. DAT occupancies of methylphenidate showed dose-dependency, and T_{max} for the profiles of DAT occupancies were 4.0, 2.0, and 2.0 min (data not shown) and plasma concentrations were 2.0 – 2.6 min, suggesting that there was little time delay between the plasma concentration profile and DAT occupancy of methylphenidate. By considering dopamine behavior in the brain and the inhibition of dopamine reuptake by methylphenidate (k_{on} and k_{off}), we developed the mechanism-based PK-PD model shown in Figure 2. The model could adequately describe the change of extracellular dopamine levels in brain (Figure 6). These results indicated that the mechanism-based PK-PD model produces optimal fit to extracellular dopamine profiles in the brain.

Discussion

For CNS acting drugs, a mechanism-based PK-PD model using biomarker responses and target receptor occupancy contributes establishment of proof of concept and pharmacological consideration by providing mechanistic information. In this aspect, a preclinical PK-PD model could be a useful tool because of limited information for biomarker responses and target receptor occupancy in humans. Since methylphenidate has been used to treat ADHD by increasing dopamine level *via* inhibition of DAT in the brain, this drug was considered appropriate for developing a mechanism-based PK-PD model. In the present study, we aimed at developing a mechanism-based PK-PD model to describe dopamine levels in the brain using k_{on} and k_{off} of methylphenidate derived from in vitro transport assay system.

Developing a methodology to determine the kinetics of drugs to receptors and transporters (k_{on} and k_{off}) offers useful information for the profiles of occupancy biomarker responses as well as pharmacodynamics (Yassen et al., 2006). For receptor kinetics, de Witte et al (2018) have already reported the analytical methodology for D₂ receptor based on the cellular response. In the present study, we focused on the transporter kinetics and a mathematical model was developed to estimate the k_{on} and k_{off} for DAT inhibitor based on high-throughput transport assay. The Neurotransmitter

Transporter Uptake Assay Kit has been used to calculate the IC_{50} of drugs to DAT at steady state (Bernstein et al., 2012). Since this system provides time-course of fluorescent strength derived from the cellular uptake of substrates to DAT, kinetic parameters of inhibitors to DAT were estimated by fitting for time-dependent uptake of substrates by DAT with the mathematical model. In the case of receptor-drug interaction, k_{on} and k_{off} can estimate using the methodology of Danhof et al. (2008) and de Witte et al (2018). According to their methodology, compound and tracer or dopamine competitively bind to the target receptor and their total amounts (or concentrations) are constant in the experimental systems. On the other hand, in the case of transporter-drug interaction, the substrate is transported into the cells in one direction and the amount (or concentration) of substrate time-dependently changes in the experimental buffer. Therefore, we established a new mathematical model including the time-dependent change of the substrate to estimate k_{on} and k_{off} for DAT based on the mechanism of DAT inhibition (equations (1) to (4)). The first-order kinetic model was selected to describe the fluorescent strength while reuptake of dopamine *via* DAT is usually explained with the Michaelis-Menten equation (Tzvetkov et al., 2013, Dave et al., 2017). The reason is that the apparent velocity (V_{app}) of the Michaelis-Menten equation can be approximated as $V_{max}/K_m \times (\text{concentration})$ when the concentration of DAT substrate is assumed much

lower than the Michaelis constant (K_m), although the actual concentration of the DAT substrate is not disclosed because of its patent. K_d values (104 nM for methylphenidate and 261 nM for cocaine), which are calculated using estimated k_{on} and k_{off} values, were comparable with published K_i values (84 ± 33 nM for methylphenidate and 120 nM for cocaine (Gatley et al., 1996) and 109 nM for methylphenidate and 210 nM for cocaine (Slusher et al., 1997)), demonstrating that the assumption is reasonable. The maximum strength of fluorescence slightly depends on sample preparation and study conditions at each examination. Therefore, C_{sub} , which explains the maximum strength of fluorescence at steady state, was treated as a variable parameter in our model. This approach can correct the inter-test variability for additional study. Human recombinant DAT was used because the rat and the human dopamine transporters are 92% homologous, the rank orders of K_i values of various dopamine uptake inhibitors at the human and the rat dopamine transporters were highly correlated and the K_i values of the methylphenidate on both species also were comparable (Giros et al., 1992).

Since the concentrations of methylphenidate in plasma were almost dose-proportionally increased after intraperitoneal administration of methylphenidate to rats, the concentrations were analyzed with a linear 2-compartment model. The absorption rate constant was also high ($k_a = 7.77/\text{min}$), presumably because the dosing

route was intraperitoneal administration and methylphenidate was dissolved in saline. Even though the calculated T_{max} using PK parameters (0.6 min) preceded the first sampling time (2 min), an absorption compartment was used for mechanistic reasons, the small CV (%) of k_a (8.18%), and the fact that the predicted values adequately described the observed data. In addition, some deviations between predicted values and observed values were obtained, especially lower concentration at low dose; however, the deviations were almost within 2-fold and then the results were acceptable. In rats, high Kp_{CSF} values (1.20-1.66) and Kp_{Brain} values (10.6-11.2) of methylphenidate were observed, suggesting that methylphenidate transfers well to the brain.

According to Aoyama et al. (1997), the estimated K_i value for methylphenidate based on extracellular fluid (ECF) was consistent with the in vitro value. In addition, our concentrations of methylphenidate in CSF were comparable with their concentration in ECF and drug concentration in CSF generally reflects the unbound concentration in ECF (de Lange EC 2013). Therefore, DAT occupancies were calculated based on CSF concentration. In addition, Patrick et al (1984) had reported there is little distributional delay to brain after intravenous administration of methylphenidate. Therefore, it was decided to construct the model with a CSF compartment attached to the central plasma compartment without time-delay distribution. The profiles of DAT occupancies

calculated with the concentration in plasma, K_p _CSF, k_{on} , and k_{off} of methylphenidate were parallel to those of plasma concentration (Figure 7). On the other hand, $T_{max,d}$ of dopamine profiles was about 4- to 13-fold of that of DAT occupancy, and then the counter-clockwise hysteresis was observed between DAT occupancies and dopamine profiles (data not shown). Then, a pharmacodynamic model including the processes of dopamine biosynthesis, release from a synapse, reuptake *via* DAT and metabolism had to be established to represent the behaviors of dopamine in the brain. The V_{max} and K_m values of the Michaelis-Menten equation for dopamine in the NAc core have been reported as 2-3 $\mu\text{M/s}$ and 0.16-0.20 μM , respectively (Budygin et al., 2007) and dopamine concentration in brain extracellular space have been reported to be 219 ± 36 pM in the hippocampus (Van Schoors et al., 2016) and 1.8 ± 0.5 nM in the medial prefrontal cortex (Faiman et al., 2013). As the dopamine concentration in the brain extracellular space was lower than K_m , the V_{app} for dopamine reuptake could be approximated as $V_{max}/K_m \times (\text{dopamine level})$. Therefore, the reuptake rate of dopamine was described by first-order kinetics as for the case where k_{on} and k_{off} of methylphenidate were calculated from the data of in vitro transport assay. The estimated k_{uptake} was about 10-fold of $k_{release}$, showing high activity for dopamine reuptake by DAT. The estimated $k_{release}$ was also much lower than k_{on} of methylphenidate, suggesting that

slow releasing of dopamine could be one of the causes for the counter-clockwise hysteresis of dopamine profiles. The CV (%) of k_{deg} was large, possibly because there was large variability in dopamine levels, especially in low dose group. In addition, our analysis revealed the relationship between DAT occupancy and DAT reuptake inhibition. The hill coefficient, which represents the degree of interaction between DAT occupancy and dopamine reuptake, was calculated as 0.578 (Table 4), indicating that non-linear increase of extracellular dopamine levels in brain to the DAT occupancy would be suggested (Figure 8). Consequently, the mechanism-based PK-PD model was successfully established by obtaining predicted dopamine profiles that were close to the observed ones following administration of methylphenidate to rats (Figure 6). This is the first analytical report related to dopamine kinetics based on target occupancy, and then the validity of these parameters would be additional evaluation using other compound with similar pharmacological mechanism to methylphenidate.

Dougherty et al. (1999) reported that DAT density in patients with ADHD was increased by 70% compared with healthy controls. Therefore, the pathological condition of the disease would also need to be considered using disease model animals, such as spontaneously hypertensive rat (Heal et al., 2008). In addition, the present PK-PD model adequately predicts the dopamine profile, but its relevance for therapeutic

outcome is currently unknown. Additional studies and mechanistic model development may be required to elucidate the relationship between dopamine profiles and therapeutic outcome. Furthermore, human pharmacodynamics could be predicted from animal data using allometry approach according to Zuidveeld et al., (2007). Our model explained the behavior of dopamine using first-order rate constants, demonstrating that our model can be scaled to one describing dopamine profiles after administration of methylphenidate to humans.

In conclusion, we successfully developed a mechanism-based PK-PD model, which accurately describes the dopamine profiles in the brain after administration of methylphenidate to rats using association and dissociation rate constants derived from in vitro transport study. These models would be useful to understand the pharmacological effects for DAT. In future study, the present PK-PD models needs to be further extended to predict therapeutic outcome for consideration of proper treatment of dopamine-related diseases such as ADHD.

Acknowledgments

The authors thank Masaaki Sato, Satoko Funaki, Hiroko Ogawa and Norihito Sato (Shionogi & Co., Ltd.) for technical assistance and many thoughtful suggestions.

Authorship Contributions:

Participated in research design: Shimizu, Horiguchi, Yano, Shinohara, Ohnishi.

Conducted experiments: Shimizu, Horiguchi, Yano, Sakuramoto, Kanegawa.

Contributed new reagents or analytic tools: Shimizu

Performed data analysis: Shimizu, Horiguchi.

Wrote or contributed to the writing of the manuscript: Shimizu, Horiguchi, Kanegawa,
Ohnishi.

Footnote

The authors, Ryosuke Shimizu, Naotaka Horiguchi, Koji Yano, Masashi Sakuramoto, Naoki Kanegawa, and Shuichi Ohnishi are full-time employees of Shionogi & Co., Ltd.

The author, Shunji Shinohara, is a full-time employee of Shionogi TechnoAdvanced Research Co., Ltd.

References

Ago Y, Sato M, Nakamura S, Baba A, Matsuda T. (2006) Lack of enhanced effect of antipsychotics combined with fluvoxamine on acetylcholine release in rat prefrontal cortex. *J Pharmacol Sci* 102:419-22.

Ago Y, Yano K, Hiramatsu N, Takuma K, Matsuda T (2011) Fluvoxamine enhances prefrontal dopaminergic neurotransmission in adrenalectomized/castrated mice *via* both 5-HT reuptake inhibition and σ 1 receptor activation. *Psychopharmacology (Berl)* 217:377-86.

Ammal Kaidery N, Thomas B. (2018) Current perspective of mitochondrial biology in Parkinson's disease. *Neurochem Int.* 117:91-113

Aoyama T, Kotaki H, Sawada Y, Iga T. (1997) Stereospecific distribution of methylphenidate enantiomers in rat brain: specific binding to dopamine reuptake sites. *Pharm Res*11:407-11.

Bernstein AI, Stout KA, Miller GW. (2012) A fluorescent-based assay for live cell, spatially resolved assessment of vesicular monoamine transporter 2-mediated neurotransmitter transport. *J Neurosci Methods* 209:357-66.

Briars L, Todd T. (2016) A Review of Pharmacological Management of Attention-Deficit/Hyperactivity Disorder. *J Pediatr Pharmacol Ther* 21:192-206.

Budygin EA, Oleson EB, Mathews TA, Läck AK, Diaz MR, McCool BA, Jones SR. (2007) Effects of chronic alcohol exposure on dopamine uptake in rat nucleus accumbens and caudate putamen. *Psychopharmacology (Berl)* 193:495-501.

Bymaster FP, Katner JS, Nelson DL, Hemrick-Luecke SK, Threlkeld PG, Heiligenstein JH, Morin SM, Gehlert DR, Perry KW. (2002) Atomoxetine increases extracellular levels of norepinephrine and dopamine in prefrontal cortex of rat: a potential mechanism for efficacy in attention deficit/hyperactivity disorder. *Neuropsychopharmacology* 27:699-711.

- Colom-Cadena M, Pegueroles J, Herrmann AG, Henstridge CM, Muñoz L,
Querol-Vilaseca M, Martín-Paniello CS, Luque-Cabecerans J, Clarimon J, Belbin O,
Núñez-Llaves R, Blesa R, Smith C, McKenzie CA, Frosch MP, Roe A, Fortea J,
Andilla J, Loza-Alvarez P, Gelpi E, Hyman BT, Spires-Jones TL, Lleó A. (2017)
Synaptic phosphorylated α -synuclein in dementia with Lewy bodies. *Brain*
140:3204-3214.
- Danhof M, Ploeger B. (2008) Implementing receptor theory in PK-PD modeling.
Population Approach Group in Europe annual meeting in 2008, Marseille, 19 June.
- Dave RA, Follman KE, Morris ME. (2017) γ -Hydroxybutyric Acid (GHB)
Pharmacokinetics and Pharmacodynamics: Semi-Mechanism-based and Physiologically
Relevant PK/PD Model. *AAPS* 19:1449–1460.
- de Lange EC. (2013) Utility of CSF in translational neuroscience. *J Pharmacokinet
Pharmacodyn.* 3:315-26

de Witte WEA, Versfelt JW, Kuzikov M, Rolland S, Georgi V, Gribbon P, Gul S, Huntjens D, van der Graaf PH, Danhof M, Fernández-Montalván A, Witt G, de Lange ECM. (2018) In vitro and in silico analysis of the effects of D2 receptor antagonist target binding kinetics on the cellular response to fluctuating dopamine concentrations. *Br J Pharmacol.*;175:4121-4136.

Dougherty DD, Bonab AA, Spencer TJ, Rauch SL, Madras BK, Fischman AJ. (1999) Dopamine transporter density in patients with attention deficit hyperactivity disorder. *Lancet* 354:2132-3.

Faiman MD, Kaul S, Latif SA, Williams TD, Lunte CE. (2013) S-(N, N-diethylcarbamoyl) glutathione (carbamathione), a disulfiram metabolite and its effect on nucleus accumbens and prefrontal cortex dopamine, GABA, and glutamate: a microdialysis study. *Neuropharmacology* 75:95-105.

Gatley SJ, Pan D, Chen R, Chaturvedi G, Ding YS. (1996) Affinities of methylphenidate derivatives for dopamine, norepinephrine and serotonin transporters. *Life Sci* 58:231-9.

Giros B, el Mestikawy S, Godinot N, Zheng K, Han H, Yang-Feng T, Caron MG.

(1992) Cloning, pharmacological characterization, and chromosome assignment of the human dopamine transporter. *Mol Pharmacol*. 42:383-90.

Heal DJ, Smith SL, Kulkarni RS, Rowley HL. (2008) New perspectives from microdialysis studies in freely-moving, spontaneously hypertensive rats on the pharmacology of drugs for the treatment of ADHD. *Pharmacol Biochem Behav* 90:184-97.

Johnson M, Kozielska M, Pilla Reddy V, Vermeulen A, Barton HA, Grimwood S, de Greef R, Groothuis GM, Danhof M, Proost JH. (2016) Translational Modeling in Schizophrenia: Predicting Human Dopamine D2 Receptor Occupancy. *Pharm Res* 33:1003-17.

Koda K, Ago Y, Cong Y, Kita Y, Takuma K, Matsuda T. (2010) Effects of acute and chronic administration of atomoxetine and methylphenidate on extracellular levels of

noradrenaline, dopamine and serotonin in the prefrontal cortex and striatum of mice. *J*

Neurochem 114:259-70.

Mereu M, Contarini G, Buonaguro EF, Latte G, Managò F, Iasevoli F, de Bartolomeis

A, Papaleo F. (2017) Dopamine transporter (DAT) genetic hypofunction in mice

produces alterations consistent with ADHD but not schizophrenia or bipolar disorder.

Neuropharmacology 121:179-194

Meiser J, Weindl D, Hiller K. (2013) Complexity of dopamine metabolism. *Cell*

Commun Signal 1:34

Moraga-Amaro R, González H, Ugalde V, Donoso-Ramos JP, Quintana-Donoso D,

Lara M, Morales B, Rojas P, Pacheco R, Stehberg J. (2016) Dopamine receptor D5

deficiency results in a selective reduction of hippocampal NMDA receptor subunit

NR2B expression and impaired memory. *Neuropharmacology* 103:222-35

Patrick KS, Ellington KR, Breese GR. (1984) Distribution of methylphenidate and

p-hydroxymethylphenidate in rats. *J Pharmacol Exp Ther.* 231:61-5.

Paxinos G, Watson C (1986) *The Rat Brain in Stereotaxic Coordinates*. (2nd ed.), Academic Press, San Diego.

Sato M, Ago Y, Koda K, Nakamura S, Kawasaki T, Baba A, Matsuda T. (2007) Role of postsynaptic serotonin_{1A} receptors in risperidone-induced increase in acetylcholine release in rat prefrontal cortex. *Eur J Pharmacol* 559:155-60.

Slusher BS, Tiffany CW, Olkowski JL, Jackson PF. (1997) Use of identical assay conditions for cocaine analog binding and dopamine uptake to identify potential cocaine antagonists. *Drug Alcohol Depend* 48:43-50.

Tzvetkov MV, dos Santos Pereira JN, Meineke I, Saadatmand AR, Stingl JC, Brockmüller J. (2013) Morphine is a substrate of the organic cation transporter OCT1 and polymorphisms in OCT1 gene affect morphine pharmacokinetics after codeine administration. *Biochem Pharmacol* 86:666-78.

Van Schoors J, Viaene J, Van Wanseele Y, Smolders I, Dejaegher B, Vander Heyden Y6, Van Eeckhaut A7. (2016) An improved microbore UHPLC method with electrochemical detection for the simultaneous determination of low monoamine levels in in vivo brain microdialysis samples. *J Pharm Biomed Anal* 127:136-46.

Visser SAG, Bueters TJH. (2017) Assessment of translational risk in drug research: Role of biomarker classification and mechanism-based PKPD concepts. *Eur J Pharm Sci* 109S:S72-S77.

Yassen A, Kan J, Olofsen E, Suidgeest E, Dahan A, Danhof M. (2006) Mechanism-based pharmacokinetic-pharmacodynamic modeling of the respiratory-depressant effect of buprenorphine and fentanyl in rats. *J Pharmacol Exp Ther* 319:682-92.

Zuideveld KP, Van der Graaf PH, Peletier LA, Danhof M. (2007) Allometric scaling of pharmacodynamic responses: application to 5-Ht1A receptor mediated responses from rat to man. *Pharm Res* 24:2031-9.

Legends for Figures

Figure 1. Scheme of the in vitro study. Figure 1[a] and 1[b] show the experiment in the absence or presence of methylphenidate, respectively. To observe the uptake of DAT substrate, which is composed of masking dye and fluorophore, the masking dye is removed and only the fluorophore is transported into the cell. Therefore, the transport activity of DAT substrate was investigated by measuring the fluorescence captured from the intracellular fluorophore. To measure fluorescence, the fluorophore was excited with light at a wavelength of 470-495 nm, and emission was collected at 515-575 nm. Each parameter was defined as follows: C_{sub} = the concentration of fluorescent substrate, C_{flu} = the fluorescent strength, C_{inh} = the concentration of inhibitor, k'_{on} (/min) = permeability rate constant for fluorescent substrate via DAT, k_{on} (/μM/min) = association rate constant of methylphenidate for DAT, k_{off} (/min) = dissociation rate constant of methylphenidate for DAT.

Figure 2. The structure of the pharmacokinetic-pharmacodynamic model for dopamine levels in the brain after intraperitoneal administration of methylphenidate. Each parameter was defined as follows: k_a = absorption rate constant, k_{12} = first-order rate constant from plasma to peripheral compartment, k_{21} = first-order rate constant from

peripheral to plasma compartment, k_e = elimination rate constant from central compartment, K_p_CSF = CSF-to-plasma concentration ratio, k_{on} = association rate constant for DAT, k_{off} = dissociation rate constant for DAT, k_{syn} = synthesis rate constant of dopamine in synapse, $k_{release}$ = first-order rate constant for dopamine release via DAT, k_{uptake} = first-order rate constant for dopamine reuptake from synapse, k_{deg} = degradation rate constant of dopamine in synapse, I_p = administration compartment, Central = central compartment, Periph = peripheral compartment, CSF = cerebrospinal flow compartment, DAT = DAT occupancy compartment.

Figure 3. The time-course of observed and predicted fluorescent strength in the absence and presence of methylphenidate. The concentrations of methylphenidate were 0.0781 - 2.50 μ M. Plots show observed data in the absence (diamonds) or presence (circles) of methylphenidate and lines show predicted data in the absence (solid) or presence (dashed) of methylphenidate.

Figure 4. The time-course of observed and predicted fluorescent strength in the absence and presence of cocaine. The concentrations of cocaine were 0.313 and 0.625 μ M. Plots show observed data in the absence (diamonds) or presence (circles) of cocaine and lines

show predicted data in the absence (solid) or presence (dashed) of cocaine.

Figure 5. The time-course profiles of observed and predicted concentrations of methylphenidate in plasma after intraperitoneal administration in wistar rats for pharmacokinetic study groups. Each symbol represents the observed mean \pm SD (n = 3-5) at 1 (open), 3 (gray), and 6 mg/kg (black), and each line represents the predicted value at 1 (solid), 3 (gray), and 6 mg/kg (dashed). [a]: normal scale and [b]: semilog scale.

Figure 6. The time-course profiles of observed and predicted dopamine levels after single intraperitoneal administration of methylphenidate to wistar rats for pharmacodynamics study groups. Each symbol represents the observed mean \pm SD (n = 4) and each line represents the predicted value at 1 [a], 3 [b], and 6 mg/kg [c].

Figure 7. Calculated occupancy for dopamine transporter after intraperitoneal administration of methylphenidate at 1 (solid line), 3 (gray line), and 6 mg/kg (dashed line).

Figure 8. The relationship between dopamine transporter occupancy and dopamine reuptake calculated using the equation: $\text{dopamine reuptake} = (1 - \text{DAT}_{\text{RO}})^\gamma$. Dashed line shows the correlation in the case of $\gamma = 1$ and solid line shows the correlation in the case of $\gamma = 0.578$ (our result)

Table 1

Estimated in vitro kinetic parameters (CV%) for fluorescent substrate and methylphenidate.

Tested concentration (μM)	C_{sub}	k'_{on} (/min)	k_{on} ($/\mu\text{M}/\text{min}$)	k_{off} (/min)	K_{d} (μM)
Control	2360 (0.32)	0.0427(0.99)	-	-	-
Methylphenidate					
0.0781			0.926 (1.72)	0.0777 (1.94)	0.084
0.156			1.20 (1.73)	0.0818 (2.23)	0.079
0.313			1.24 (3.66)	0.129 (4.28)	0.104
0.625	-	-	2.31 (2.76)	0.250 (2.90)	0.108
1.25			1.14 (2.53)	0.146 (2.78)	0.128
2.50			0.810 (3.71)	0.122 (4.19)	0.151

Cocaine				
0.313		0.492 (1.34)	0.123 (1.64)	0.250
0.625	-	0.512 (1.55)	0.134 (1.67)	0.261

Each parameter was defined as follows:

C_{sub} = the concentration of fluorescent substrate, k'_{on} (/min) = permeability rate constant for fluorescent substrate *via* DAT,

k_{on} (/μM/min) = association rate constant of methylphenidate or cocaine for DAT,

k_{off} (/min) = dissociation rate constant of methylphenidate or cocaine for DAT,

K_d (μM) = dissociation constant for methylphenidate or cocaine and calculated as $k_{\text{off}} / k_{\text{on}}$

Table 2

Pharmacokinetic parameters of methylphenidate in plasma after single intraperitoneal administration of methylphenidate to rats

Dose (mg/kg)	C_{max} (ng/mL)	AUC_{inf} (ng·hr/mL)	T_{max} (min)	Kp_{brain}	Kp_{CSF}
1	139 ± 42.5	39.0 ± 7.96	2.0 ± 0.0	10.6 ± 0.85	1.31 ± 0.13
3	435 ± 84.2	166 ± 0.727	2.0 ± 0.0	11.2 ± 1.23	1.20 ± 0.04
6	1030 ± 143	372 ± 53.5	2.6 ± 1.3	11.2 ± 1.07	1.66 ± 0.19

Data represent mean ± SD (n = 3-5)

Table 3

Pharmacodynamic parameters of methylphenidate in microdialysate after single intraperitoneal administration of methylphenidate to rats

Data represent mean \pm SD (n = 4)

Dose (mg/kg)	L_{max_d} (% of baseline)	dAUE_{all} (% of baseline*min)	T_{max_d} (min)
1	260 \pm 132	7633 \pm 8385	25.5 \pm 22.7
3	346 \pm 110	9418 \pm 3216	19.5 \pm 13.3
6	455 \pm 72.5	20324 \pm 4414	16.5 \pm 7.55

Table 4

Parameters of methylphenidate estimated by mechanism-based pharmacokinetic and pharmacodynamic model.

Parameter	Definition	Estimate	CV (%)
k_a (/min)	Absorption rate constant	7.77	8.18
k₁₂ (/min)	First-order rate constant from plasma to peripheral compartment	0.0141	38.5
k₂₁ (/min)	First-order rate constant from peripheral to plasma compartment	0.0330	27.2
k_e (/min)	Elimination rate constant from central compartment	0.0551	7.34
V_d/F (L/kg)	Distribution volume of methylphenidate in the central compartment	5.59	8.03
K_{p_CSF}	CSF-to-plasma concentration ratio	1.25	Observed
k_{deg} (/min)	Degradation rate constant of dopamine in synapse	0.0282	121
k_{release} (/min)	First-order rate constant for dopamine release <i>via</i> DAT	0.0629	49.8

k_{uptake} (/min)	First-order rate constant for dopamine reuptake from synapse	0.533	20.3
γ	Hill coefficient	0.578	8.18

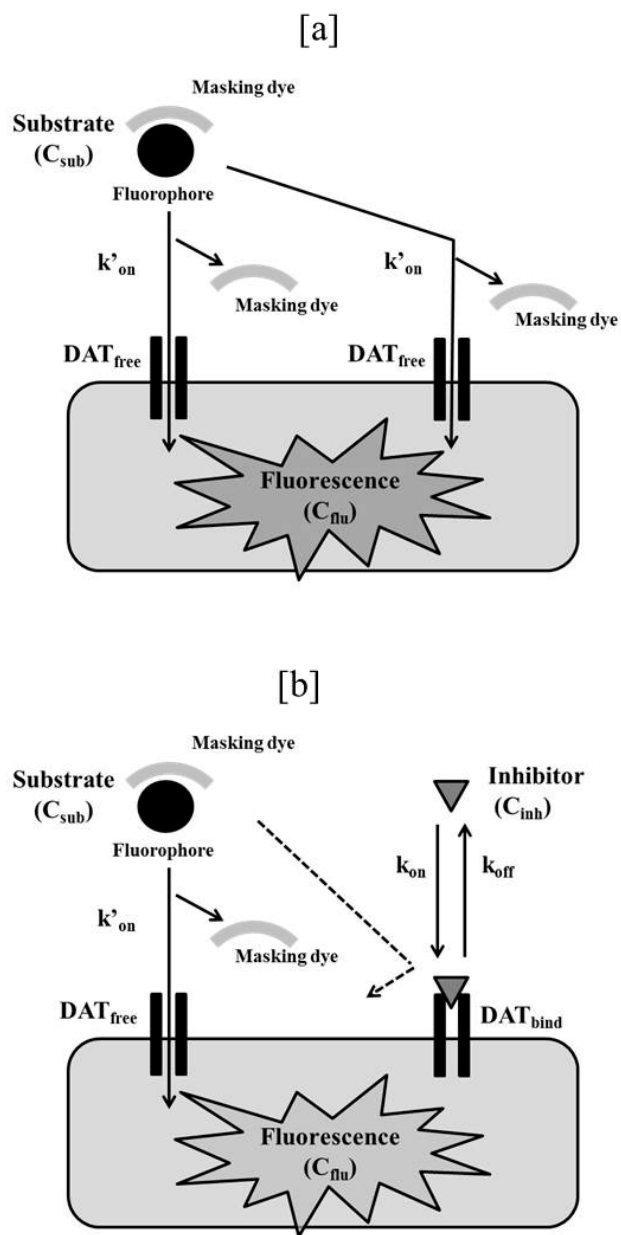


Figure 1.

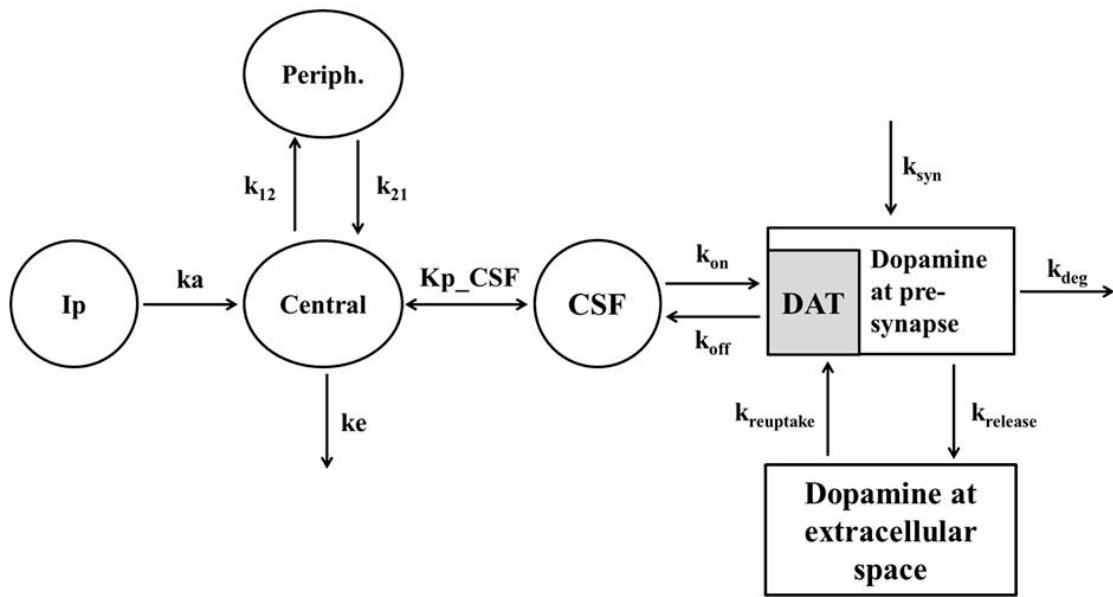


Figure 2.

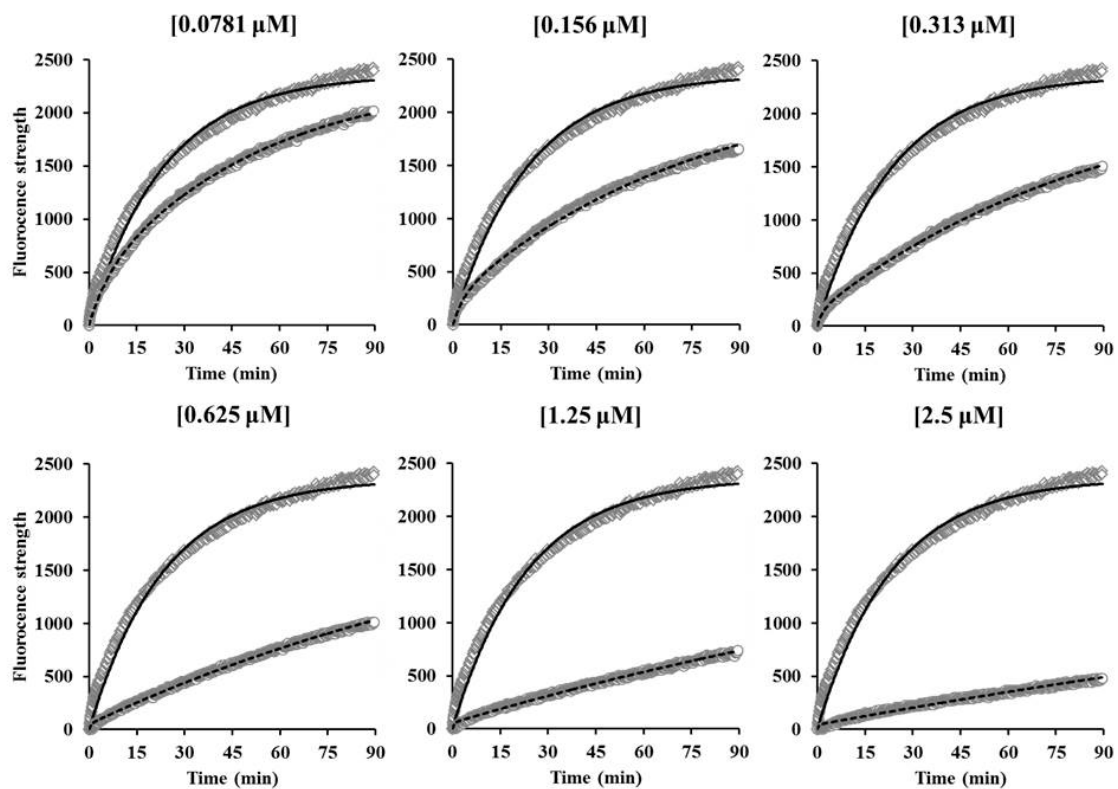


Figure 3.

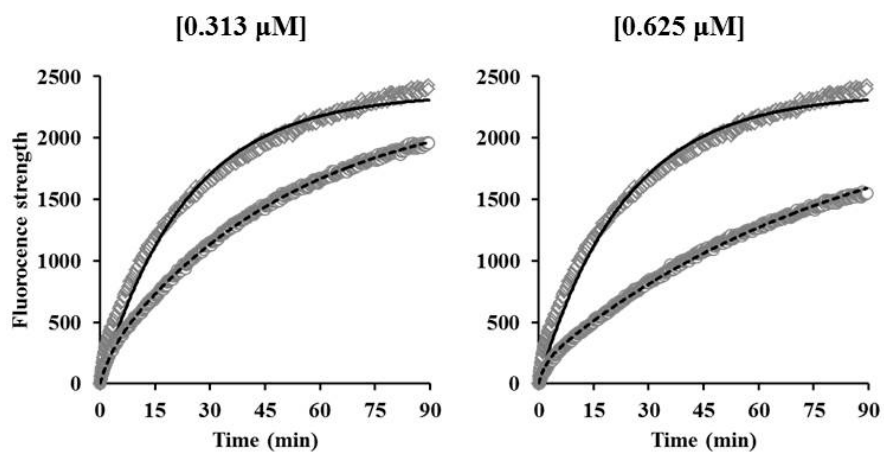


Figure 4.

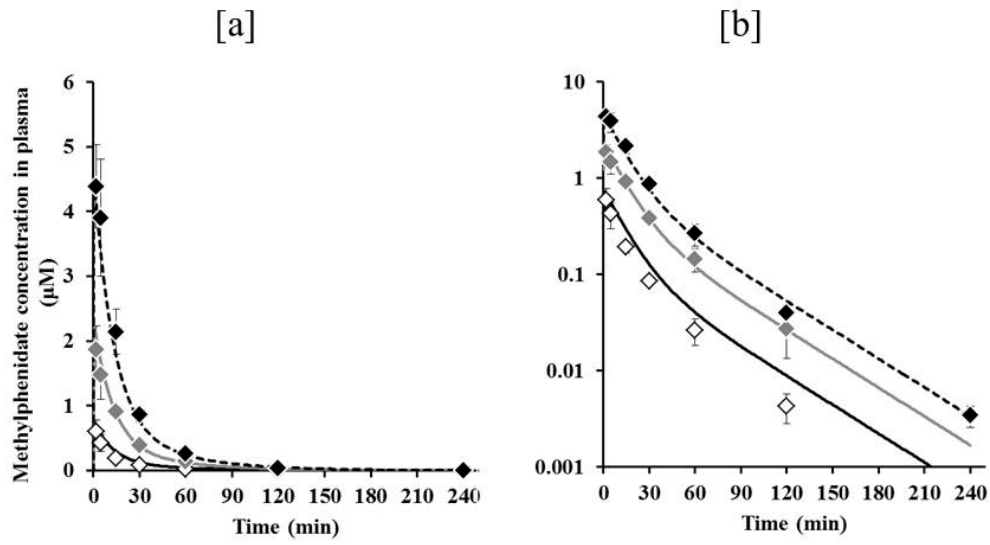


Figure 5.

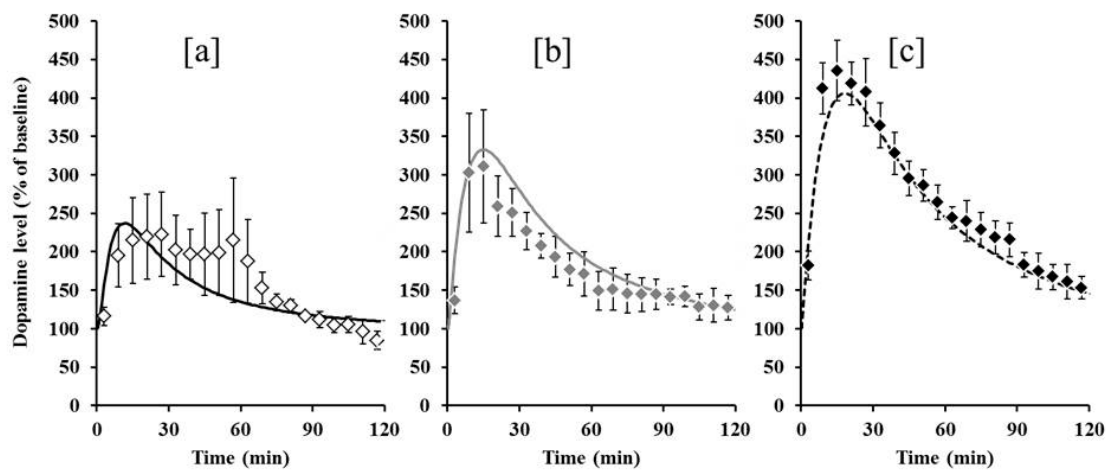


Figure 6.

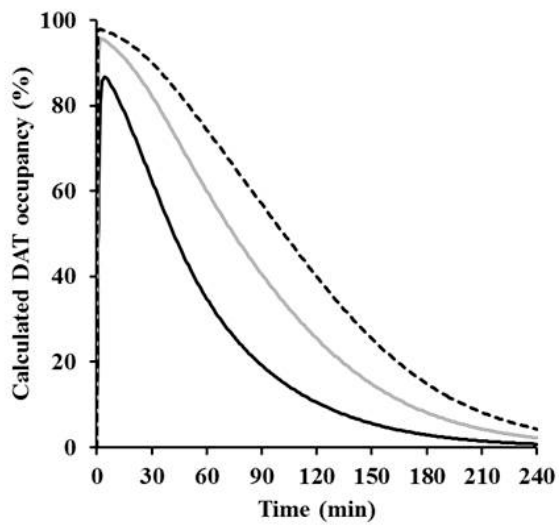


Figure 7.

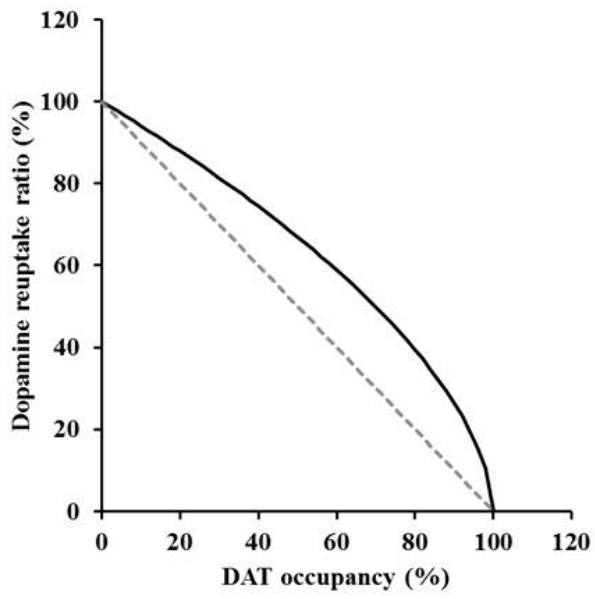


Figure 8.